Journal of Material Cycles and Waste Management (2023) 25:2822–2834
https://doi.org/10.1007/s10163-023-01710-y

ORIGINAL ARTICLE

Some investigation on ternary powder (binder) technology incorporated with ferrochrome slag as fine aggregate in concrete

Manigandan Nagarajan[1] · **Ponmalar Vijayan**[1]

Received: 2 February 2023 / Accepted: 14 May 2023 / Published online: 24 June 2023

Abstract

The supplanting of fine aggregate was encapsulated in this study to reduce the usage of non-renewable materials in concrete. Initially, nano–micro cementitious material (NMCM) such as metakaolin (MK) and nano silica (NS) was incorporated with Portland cement to make referral concrete (RC). An alternate for virgin river sand is crushed gravel sand (Csand) which is mostly in use. The objective of this research is to effectively supplant Csand by means of ferrochrome slag (FS). Precisely, the optimum level of MK (10%) and NS (1%) was used in place of cement. In addition, the FS was incorporated in place of Csand by 10, 20, 30, 40, 50 and 100%. A significant rise in the compressive strength of about 3.18% was achieved by replacing FS4 at 28 days than RC. Ultrasonic pulse velocity (UPV) and water permeability (WP) results of FS4 were better than those of RC. F4 was 12.5% higher in the RCPT result than for the RC specimen. The SEM image of FS4 indicates the densest calcium silicate hydrate (CSH(H)) and rigidified interfacial transition zone (ITZ). TG/DTG predicts that the FS4 mix has a minimal Portlandite (CH-3.92%) compared to RC. The strength, durability, microstructure and TG results of the FS4 matrix imply that FS can be substituted for fine aggregate.

Extended author information available on the last page of the article

Graphical Abstract

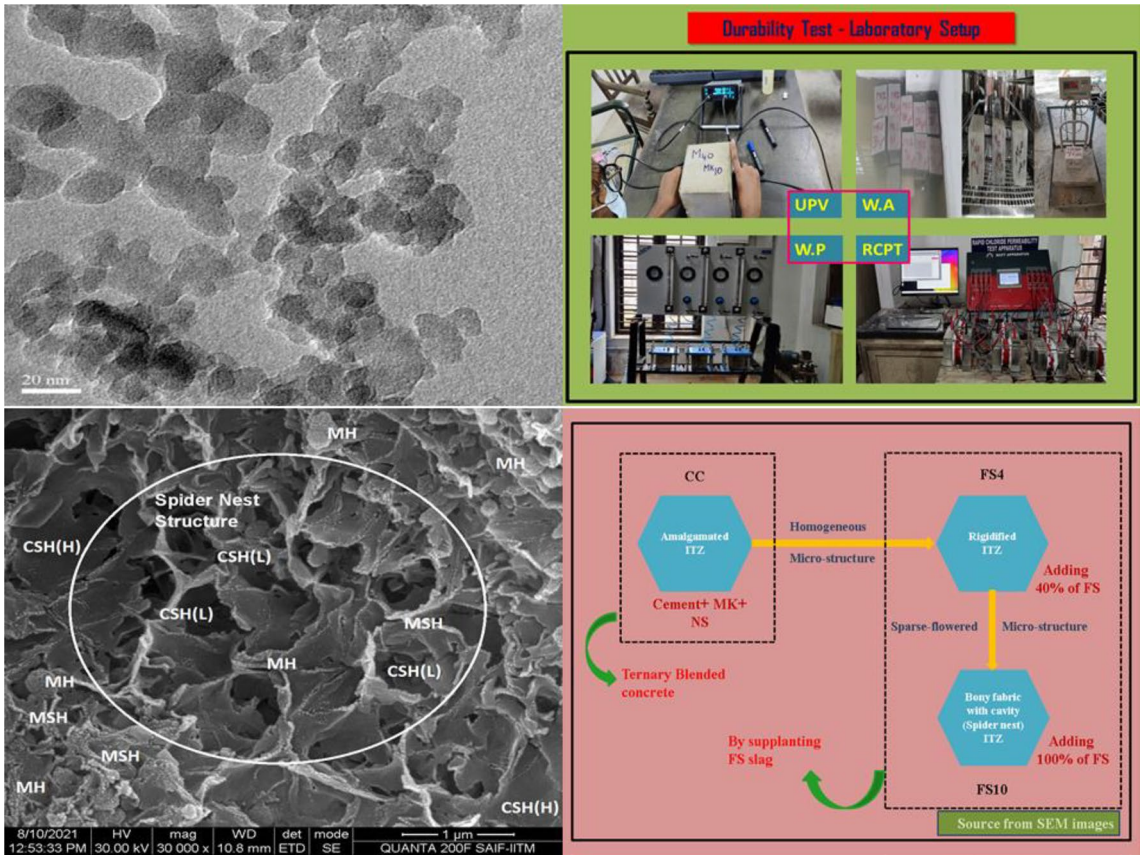

Keywords Ferrochrome slag · Durability · RCPT · UPV and ITZ

Introduction

Nano–micro cementitious material (NMCM)

Industrialization, urbanization and modernization exploit a massive amount of natural resources. Development should be sustainable and environmentally free from harm. In the civil engineering firms, the clinker process causes major harm to ecology. The 10% of world CO_2 emission is contributed by cement production. And this negative consequence are overcomed by NMCM [1, 2]. Cement for binder and Csand for fine aggregate are used extensively in India for concrete production. This causes a *dwindling effect* on the source of cement and Csand. Therefore, an alternative cementitious system (ACS), such as MK, NS, fly ash, silica fume, rice husk ash, GGBS and other natural and industrial waste pozzolans, is used instead of ordinary Portland cement (OPC) [3, 4]. These minerals strengthen the matrix by reducing OPC besides reducing pollution in society. MK as a micro pozzolans and NS as nano pozzolans are used in NMCM replacement.

Al–Si is an MK mineral of amorphous nature. MK is formed by dehydroxylation of kaolinite at 650–800ºC [5]. Al–Si in MK makes the structure dense by eradicating the amount of CH [Ca $(OH)_2$] and increasing CSH (or) calcium aluminosilicate hydrate [C(A)SH]. This is due to the rigours *potential pozzolanic mechanism* and *micro filler mechanism* of MK [5–7]. Codal provision and antecedent exploration of MK ranges from 5 to 15% weight of cement. As the Al/SO_3 ratio increases in MK, ettringite (Aft) is converted to monosulfate aluminate (Afm). MK at 10% weight of binder makes the microstructure homogeneous and contributes to rapid strength [8, 9]. RCPT, water absorption (WA), and the pores are reduced by adding 4% of nano-MK to concrete. Increase in CSH leads to

the densest microstructure. MK rigorously performs with cement as a good pozzolan [10].

NS is a nano-ranged mineral that refines the capillary pore and forms secondary CSH by reducing CH content. Moreover, amorphous nano-sized silica is majorly available in two forms: powder NS and colloidal NS. MK of 10% and NS of 3% have good hardened strength property, due to the reduction of the Ca/Si ratio in the concrete cluster. A tremendous amount of CSH is witnessed in the microstructural study of NS along with the MK matrixes [11]. ITZ of the NS matrix has a compact and uniform microstructure. The *nano filler mechanism* and *kinetic pozzolanic mechanism* of NS clog the capillary pore. Investigation of 0.3 and 0.9% NS reveals that 0.3% performs better than 0.9% NS due to superfluity and agglomeration. RCPT and WA results are reduced by adding an optimum amount of NS [12].

Higher surface area NS consumes more superplasticizer (SP) to maintain its workability. *Hydrophobic action* of SP like polymer base chemical is used in the nano concrete [13]. The addition of NS increases the average chain length of CSH. The amount of CH is also reduced by NS [14]. Due to the self-desiccation of NS, there is autogenous shrinkage, which is overcome by adding an optimum level of SP and water. NS reduces permeability and WA inside the concrete [15, 16]. High-density CSH [CSH(H)] and low-density CSH [CSH(L)] are explained using the microstructure of Portland cement. Therefore, the CSH(L) has a low compact form of silicate hydrate (Reticular Networking System) with a discontinuity structure (hadley grains), thus the CSH(H) is more stable than CSH(L) [17].

Fine aggregate

Total aggregate occupies 70% of concrete, whereas fine aggregate consumes 45%. Based on United Nations Environmental Programme (UNEP), 50 billion tonnes of river sand is required per annum. A complete ban on river sand mining is the reason for enormous Csand production. The exploitation of the hilly region has occurred in Csand manufacturing. According to the Tamil Nadu Public Work Department (TNPWD), 12 million cubic feet of fine aggregate is utilized daily for Tamil Nadu state development alone [18]. Economically, Csand is better than virtual river sand. The quality of Csand depends on the crushing shaft, geo-features of raw material, grading and bucket wash. Csand, another name of manufactured sand, is replaced with offshore sand by 0, 25, 50 and 75%. Fresh and hardened properties of 25% Csand replacement are significant [19]. Micro-fines (< 75 µm) in Csand were investigated in this study. Moreover, 4.3–20% of micro-fines in Csand will not affect the strength of concrete. With the increase in the surface roughness of Csand, there is an increase in the crushing value of concrete.

Csand has superior roughness than river sand. There is a less significant effect of Csand roughness on its strength. Proper Csand manufacturing process can contribute to a higher mechanical strength of concrete. Ultrahigh strength concrete (UHSC) is prepared with Csand instead of natural sand. The microstructure of Csand matrix shows a very finer hydration component to enhance the performance of concrete. UHSC with Csand contributes to the strength witnessed from energy-dispersive spectroscopy (EDS) and mapping of elements [20, 21]. HSC with Csand is achieved and thermogravimetric (TG) of Csand matrix reduces the little amount of CH in concrete. The interlocking property of Csand plays a role in the microstructure and strength of HSC. However, an alternate finding on Csand is not yet concluded [22].

For both high and low grade of concrete production, Csand is used in this investigation. Higher paste volume is required to attain flow using Csand in the place of river sand. Proper grading of crushed sand can be utilized in both grades of concretes [23]. Csand requires a higher SP content than river sand concrete to attain the same amount of slump. Both Csand and river sand concrete show nearly equal modulus on the 28-day result. Granite, dolomite and limestone were compared to river sand. Moreover, the transition zone on granite Csand is denser than other rocks as fine aggregate in HSC [24]. Embodied CO_2 emission and embodied energy of 40% and 60% ceramic fine aggregate perform better. From an economic point of view, 100% ceramic can be used as a fine aggregate without affecting the target mean strength [25].

Based on the International Chromium Development Association (ICDA), FS is produced worldwide in ferro alloy industries (14–15 million tonnes /year). For every tonne of ferrochrome ore production, nearly 1.1 tonnes of FS is expelled [26, 27]. Heaps of waste FS consume a large area of landfills. FS with river sand contributes to strength at later ages and delays strength at the early age of the test. This action is due to the Mg content of slag. Partial replacement of FS increases strength gain. The partial combination always contributes to better *interlocking action* and high specific gravity. Complete replacement of FS as fine aggregate causes degradation of strength. MSH and MH are formed in the FS slag matrix that causes antagonistic activity on strength and durability [28, 29]. The microstructure of FS as a fine aggregate matrix shows a uniform CSH formation at 20–50% replacement [30]. Slag with metals causes an increase in water absorption and chloride ion penetration because some conductive metals are ingredients [31–33]. TG/DTG analysis was studied to calculate the amount of carbonation and hydroxylation on concrete. Quantification of CH was reduced by adding Si-–Al based pozzolans [34–36].

Novelty and gap findings

Precursors explored that FS utilized as macadam material and coarse aggregate in concrete. Moreover, NMCM as a binder and fine aggregate replacement of FS that competes with Csand is the novelty of this investigation. Nevertheless, a ternary combination of NMCM with FS has not been explored so far. Radically the longer age durability, strength and thermal behaviour of FS are illustrated in this probing.

Material characterization and methodology

OPC 53 grade cement was used as per the Indian standard 12,269:1987(R2013) [37]. The specific gravity of cement is 3.14. Calcined kaolinite sintered at 450–600 °C displays the amorphous phase of aluminosilicate. MK's specific gravity and bulk density are 2.6 and 450 (g/lit). Figure 1a shows

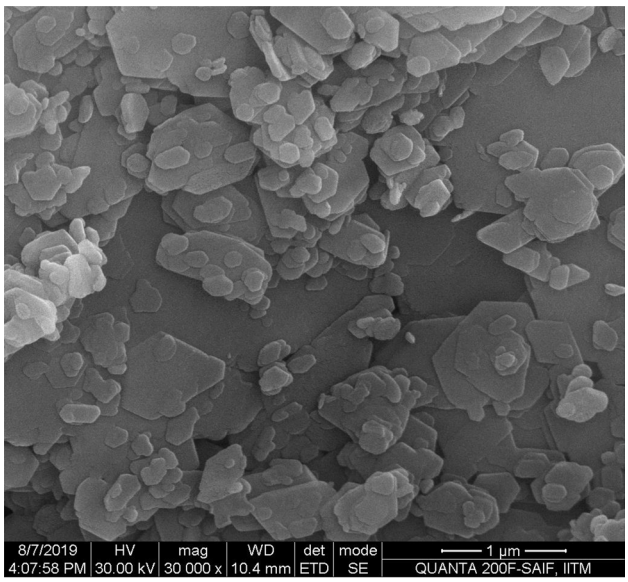

(a) SEM image of MK

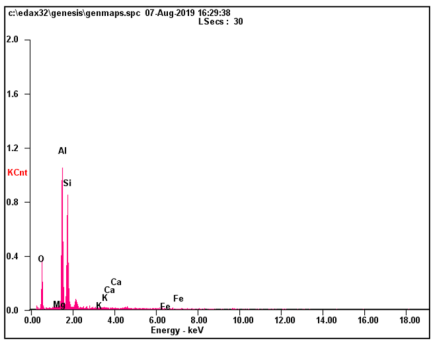

(b) EDS of MK

Fig. 1 **a** SEM image of MK. **b** EDS of MK

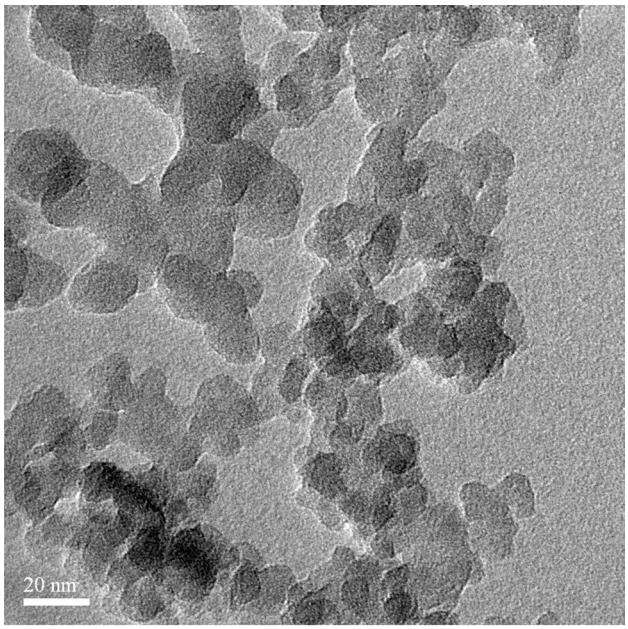

(a) TEM image of NS

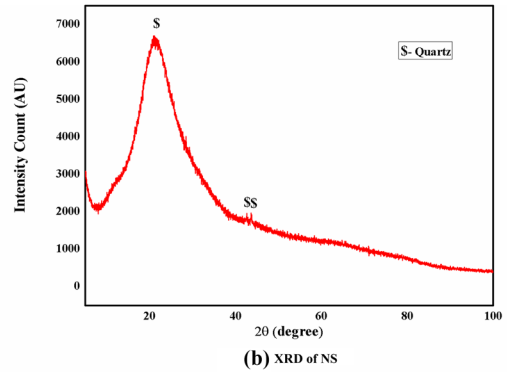

(b) XRD of NS

Fig. 2 **a** TEM image of NS. **b** XRD of NS

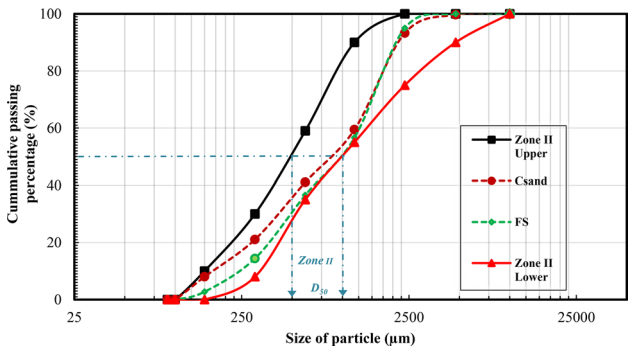

Fig. 3 Particle size distribution of fine aggregate

MK with flaky and hexagonal shape in microscale. Figure 1b shows MK illustrating the availability of the chemical element. Al and Si are predominant elements predicted in EDS. MK is sticky in nature and off-white in colour.

NS in powdered form is foggy in nature and milky-white in colour. Figure 2a portrays the TEM image of NS, which looks like an interlinked chain with high angle grain boundaries (HAGB) at a converging spot. XRD of NS confirms that the amorphous phase of SiO_2 is superior, which is available in the mineral form of quartz, as illustrated in Fig. 2b. However, Fig. 3 illustrates that both grained FS and Csand fall inside Zone II sand. The S-curve shows well-graded crushed sand. FS and Csand have a specific gravity of 2.91 and 2.67, respectively. The fineness modulus is 2.9 and 2.77 with a bulk density of 1898 (kg/m^3) and 1590 (kg/m^3), as represented in Table 1 according to IS 2386 (2) (1963) [38]. Grained FS shows a higher specific gravity, bulk density and surface roughness than Csand.

The methylene blue value (MBV) of fine aggregate should be less than 1 as per BS EN 933-9 (2010) [39]. FS and Csand have an MBV of 0.5 and 0.35, respectively. To the naked eye, the FS texture is rough and gloomy grey, and Csand is crumbly in nature and grey in colour. The SEM image of FS looks like an irregular cluster (Fig. 4a. The EDS of FS demonstrates the Si, Al, Mg, Cr, Ca and Fe elements (Fig. 4b. A Pan mixture of 40L capacity is used to make concrete. Specimen sizes of 150*150*150 mm cube are used to study the crushing strength, UPV, WP, and WA of concrete test at different ages. For RCPT, 100*50 mm diameter and height specimens are used to test the respective ages. The pore nature of slag affects the long-term serviceability. Therefore, to check durability characteristics of FS concrete by conducting WP, UPV, WA and RCPT tets.

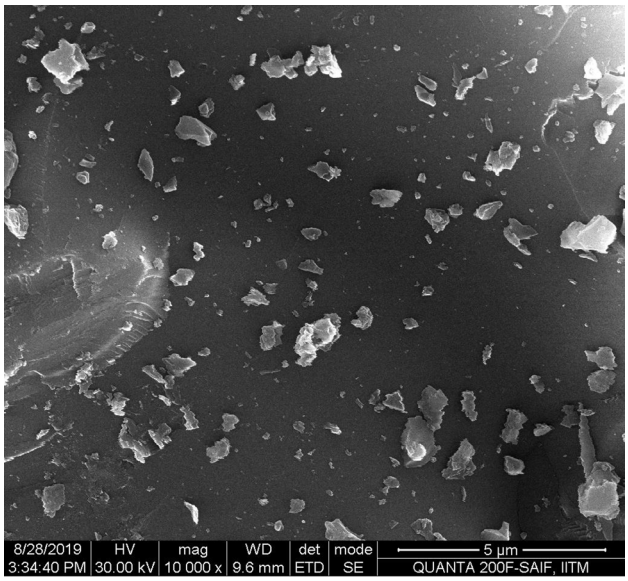

(a) SEM image of FS

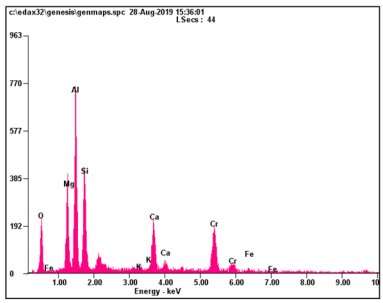

(b) EDS of FS

Fig. 4 **a** SEM image of FS. **b** EDS of FS

Mix design and workability

Mix proportion

The concrete mixtures are designed as per IS 10262: (R2019) to produce M40 grade of concrete [40]. In the

Table 1 Physical study on ingredients

Properties	NS	MK	FS (<4.75 mm)	Csand (<4.75 mm)
Appearance	Milky white	Off-white	Gloomy grey	Grey
Nature	Foggy	Sticky	Rough and porous	Crumbled sand
Specific gravity	2.2	2.6	2.91	2.67
Specific surface area (m^2/g)	202	19	–	–
Fineness modulus	–	–	2.9	2.77
Bulk density	50 (g/lit)	450 (g/lit)	1898 (kg/m^3)	1590 (kg/m^3)
Visualized texture	Nano grain powder	Micro grain powder	Porous sand	Crushed granite
Electron microscope (texture)	HAGB with interlinked chain	Hexagonal shape and flat	Irregular cluster	–
Grading	–	–	Zone II	Zone II
MBV (<)1	–	–	0.5	0.35

Table 2 Mix proportion (M40)

Sample ID	Mix proportion	Binder (kg/m^3)			Fine aggregate (kg/m^3)		Coarse aggregate (kg/m^3)		SP (%)	w/b	Attained Slump (mm)
		OPC	MK	NS	Csand	FS	18 mm	12 mm			
RC	MK10NS1	356.4	40	3.6	812.1	–	319.9	746.59	0.75	0.4	100
FS1	MK10NS1-10FS	356.4	40	3.6	730.89	81.21	319.9	746.59	0.75	0.4	100
FS2	MK10NS1-20FS	356.4	40	3.6	649.68	162.42	319.9	746.59	0.75	0.4	90
FS3	MK10NS1-30FS	356.4	40	3.6	568.47	243.63	319.9	746.59	0.75	0.4	85
FS4	MK10NS1-FS40	356.4	40	3.6	487.26	324.84	319.9	746.59	0.75	0.4	80
FS5	MK10NS1-FS50	356.4	40	3.6	406.05	406.05	319.9	746.59	0.75	0.4	75
FS10	MK10NS1- FS100	356.4	40	3.6	–	812.1	319.9	746.59	0.75	0.4	45

present study, Table 2 depicts the mixed proportion of all percentage replacements. Coarse aggregate (CA) or granite gravel of 18 mm and 12 mm are used at 30:70 proportions per IS 383:2016, which is constant throughout all the mixes [41]. Sulphonated naphthalene polymer (SNP) with a specific gravity of 1.18 is used as SP. This chemical admixture is chloride free and brown in colour. SNP led to a *hydrophobic mechanism* with ingredients to accelerate the workability of fresh concrete.

The arrived mix proportion is 1:2.03:2.67. The water binder ratio (w/b) is 0.4% and an SP of 0.75% is constantly maintained for all mixes. With RC as binder optimum, 10, 20, 30, 40, 50 and 100% of FS replacements are indicated as FS1, FS2, FS3, FS4, FS5 and FS10, respectively.

Mixing methodology

Uniform dispersion of NS in concrete majorly depends on batching and blending. The NS powder is stirred for 90 s to make a fluid state with water and SP. Prior to the addition of NS, SP and water are stirred for 15 s. A stainless steel agitator is used to make a uniform dispersion. Totally, 4–6 min of mixing is required to make good concrete as per IS 4925(2004) [2, 42]. All the mixes take 5:30 (1:45 + 3:45 min) min of cumulative mixing time of concrete. Therefore, the concrete is cured under water for the respective test days.

Fresh property

The control mix has a 100 mm slump. Degrading in workability occurs by supplanting FS in concrete. In FS4 and FS10, the slump ranges from 80 and 45 mm, respectively. Physical study confirms that the rough texture and porous nature of FS tend to reduce the fresh properties of M40 concrete. This study has a constant w/b and SP to investigate the performance of each mix. By increasing the FS level incorporation, there is a decrease in workability. This can be overcome by making correction in the SP and w/b ratio [51].

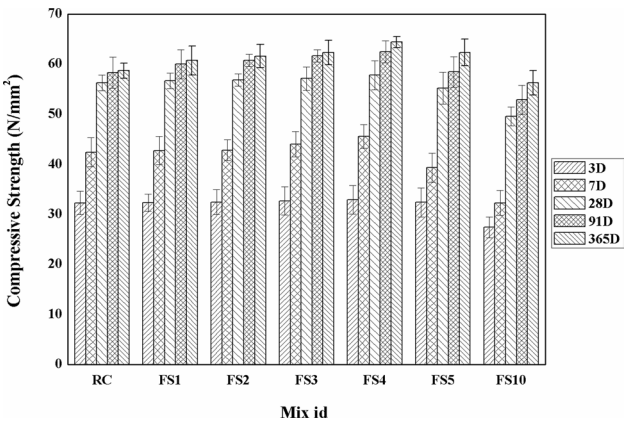

Fig. 5 Compressive strength

Fact findings

Compressive strength

The cured concrete cubes are crushed on 3, 7, 28, 91 and 365 days, respectively. Compressive strength is visualized in Fig. 5. The referral mix (RC) has a compressive strength of 55.93 N/mm^2 at 28 days. Aluminium–silica is predominant in MK and NS. However, NMCM eradicates CH and forms C(A)SH. By increasing silicate hydrate and aluminium hydrate, the concrete gets denser and superior in strength. Nevertheless, fine aggregate replacement by FS is done instead of Csand in the mix. FS1 to FS4 have no degradation of compressive strength at all ages. On 28-day tests, FS4 shows a 57.77 N/mm^2. From Fig. 5, the later age strength of the FS matrix shows an increase. 40% of FS and 60% of Csand result in a better *interlocking mechanism* of the aggregate and binder [50]. The same FS4 mix shows higher compressive strength on the 91 and 365 days, where the corresponding test values are 62.45 and 64.38 N/mm^2. This is due to the presence of Mg in slag. FS5 and FS10 mixes show lesser strength. The increase of FS causes an increase of Mg

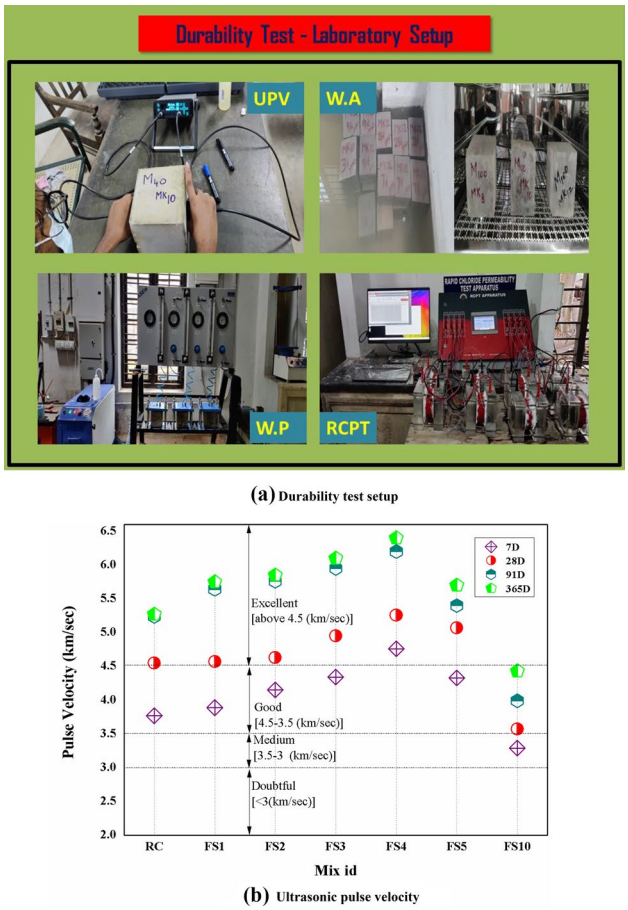

Fig. 6 **a** Durability test setup. **b** Ultrasonic pulse velocity

in concrete. Higher Mg delays early strength and hydrates later. However, the FS10 mix on 28-days crushing value is lesser than the referral mix. Nevertheless, FS10 lies below the RC strength. Mg in the FS matrix reacts to form MSH and brucite (MH).

Durability studies

The durability test relates to the service life of concrete. Moreover, UPV, WP, WA and RCPT tests were investigated in the laboratory as per Fig. 6a durability test setup.

Ultrasonic pulse velocity (UPV)

The ultrasonic pulse velocity of 150 mm cube was tested after curing on 7, 28, 91 and 365 days, respectively, to detect the velocity. According to IS 1131 (1992) part I, piezoelectric transducer was used. The quality of concrete using pulse velocity above 4.5, 4.5 to 3.5, 3.5 to 3 and below 3 km/s is, respectively, excellent, good, medium and doubtful concrete [43]. The compressive strength of concrete is almost similar to all the UPV results. By replacing 40% slag, there is higher velocity in both early and later ages. A dense structure allows the pulse velocity to pass faster. From Fig. 6 b), FS4 on 7-day test has a 4.76 km/s. On 7-day test of sample id RC, FS1, FS2, FS3 and FS5 belong to a good range of concrete.

RC to FS5 showed excellent quality of concrete on 28-day test. The FS4 mix stimulates a velocity of 5.26 km/s at 28 days. FS10 mix on 28-day test has a velocity of 4.28 km/s, which falls under a good quality of concrete as per the IS code. There is not much variation in RC on 91 and 365 days of test results. All the FS mixes at 91- and 365-day test showed an increase in velocity on passing through concrete. This confirms that the hydration of the NMCM mix occurs mostly at early ages (e.g. RC), which is similar to mechanical strength behaviour. Mg in slag reacts at a later age. FS4 had 6.4 km/s on the 365-day result. FS5 and FS10 mixes had a sliding face of velocity in all the test ages. FS10 has a velocity of 4.43 km/s on 365 days of the cured specimen and even lays on a good grade of concrete. The FS10 mix is non-homogeneous. This is witnessed from the SEM image (Fig. 10d) and this is the reason for the fall in the passing pulse velocity.

Water permeability (WP)

The 150 mm cube specimens were cured for the respective days to test as per IS 3085: 1965. Each sample was continuously pressured at 10 kg/cm^2 for 72 h before splitting and measuring the penetration depth [44]. On 28 days, cured referral concrete (RC) had a water penetration depth of 19 mm. On 91 and 365 days, RC has a 12 and 11 mm penetration depth. This emphasizes that there is no more hydration at a later age of the control mix, which is similar to the strength behaviour. MK and NS in the matrix reduce the water permeability depth, because it makes the concrete dense and reduces porosity. Meso-capillary pores are refined by adding MK and NS and make the concrete dense. NMCM in concrete increases the strength and durability property. Regard to slag replacement the penetration depth of water is reduced until FS4 mix. The FS1, FS2, and FS3 blends makes a depth of penetration of 18, 17 and 15 mm on 28 days specimen. The FS4 on 28, 91, and 365 days has a 12, 9 and 7 mm depth of water penetration after 72 h. The *interlocking mechanism* between Csand (60%) and slag (40%) causes uniformity in the heterogeneous matrix [50]. This heals the ITZ and strengthens the concrete. FS5 and FS10 show an increase in water depth penetration due to increase in slag percentage. The FS10 mix allows 39, 32 and 27 mm depth of water penetration. Mg reacts later and arrests the water penetration in 91 and 365 days on FS replacement. Hydration at a later age contributes to strength and durability in a later period, as illustrated in Fig. 7.

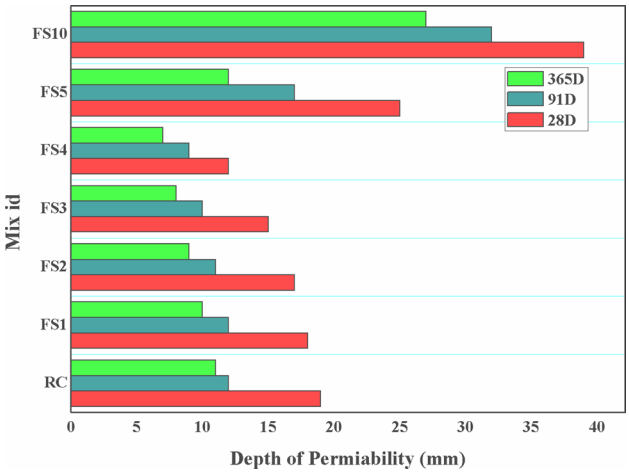

Fig. 7 Water permeability

Water absorption (WA)

Cube moulds of 150 mm are used to investigate the water absorption of concrete as per ASTM C 642-13. The specimens are tested on 7, 28, 91 and 365 days of curing. The masses of wet and oven-dried specimens are used to measure water absorption of solid mould. Oven-dried temperature is maintained around 110 ± 5 °C for 72 h and kept at room temperature for 24 h and weighed (dry weight) [45]. Following the same procedure, the samples are immersed in water for 48 h and weighed (wet weight). WA of the referral mix (RC) shows nearly 1.608, 1.4, 1.37 and 1.34%, respectively, on the 7, 28, 91 and 365 days. The *filler mechanism* and *pozzolanic mechanism* of MK and NS reduce the WA and contribute to excellent concrete strength.

FS supplanting shows a slight increase of WA in both early and later ages. FS4 has a WA of 2.32%, 2.2%, 1.98% and 1.7% on 7, 28, 91 and 365 days, respectively. Based on strength and other durability reports, WA should be decreased, yet the FS4 replacement shows slightly higher WA. However, the porous nature of slag helps to absorbs water and store it. Moreover, water absorption is material dependent (pore surface) and permeability is structural dependent (continuity of pore). From current investigation result, WA is higher than WP. FS10 shows a 4.43%, 4.32%, 3.9% and 3.62% of WA on the respective days of testing. Figure 8 represents slag replacement with fine aggregate. The porous texture of FS is the reason for the increase of WA and will not affect much the strength when the allowable limit of water in the concrete is 10%. Continuity of pores is not found in FS4, and it can be witnessed from the SEM image (Fig. 10d of FS10.

Rapid chloride penetration test (RCPT)

According to ASTM C1202-2019, RCPT tests are conducted on the cured samples on the 28, 91 and 365 days by applying a potential of 60 V. The chloride ions (Cl^-) can pass on 50 mm width and 100 mm diameter concrete for 6 h. Results are segregated into five ranges. They are categorized as above 4000, 2000–4000, 2000–1000, 100–1000 and below 100 Coulombs [46], and named, respectively, high, moderate, low, very low, and negligible chloride ion penetration. The RC is 880, 840 and 820 Coulombs for 28, 91 and 365 days cured specimen. The C(A)SH formation in concrete allows a very low amount of Cl^- ions to penetrate into RC. Meso and micro capillary pores are apprehended by micro-nano particles. Moreover, the amorphous nature of NS and MK contributes to forming an enormous amount of CSH and dense microstructure. This interrelates almost similarly to the strength, durability and microstructure of concrete.

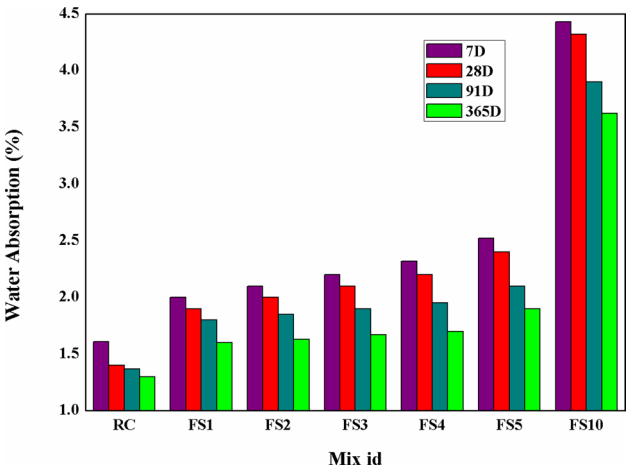

Fig. 8 Water absorption

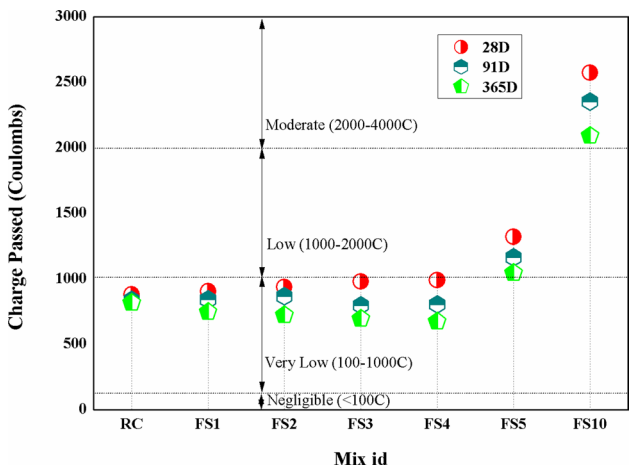

Fig. 9 Rapid chloride penetration test

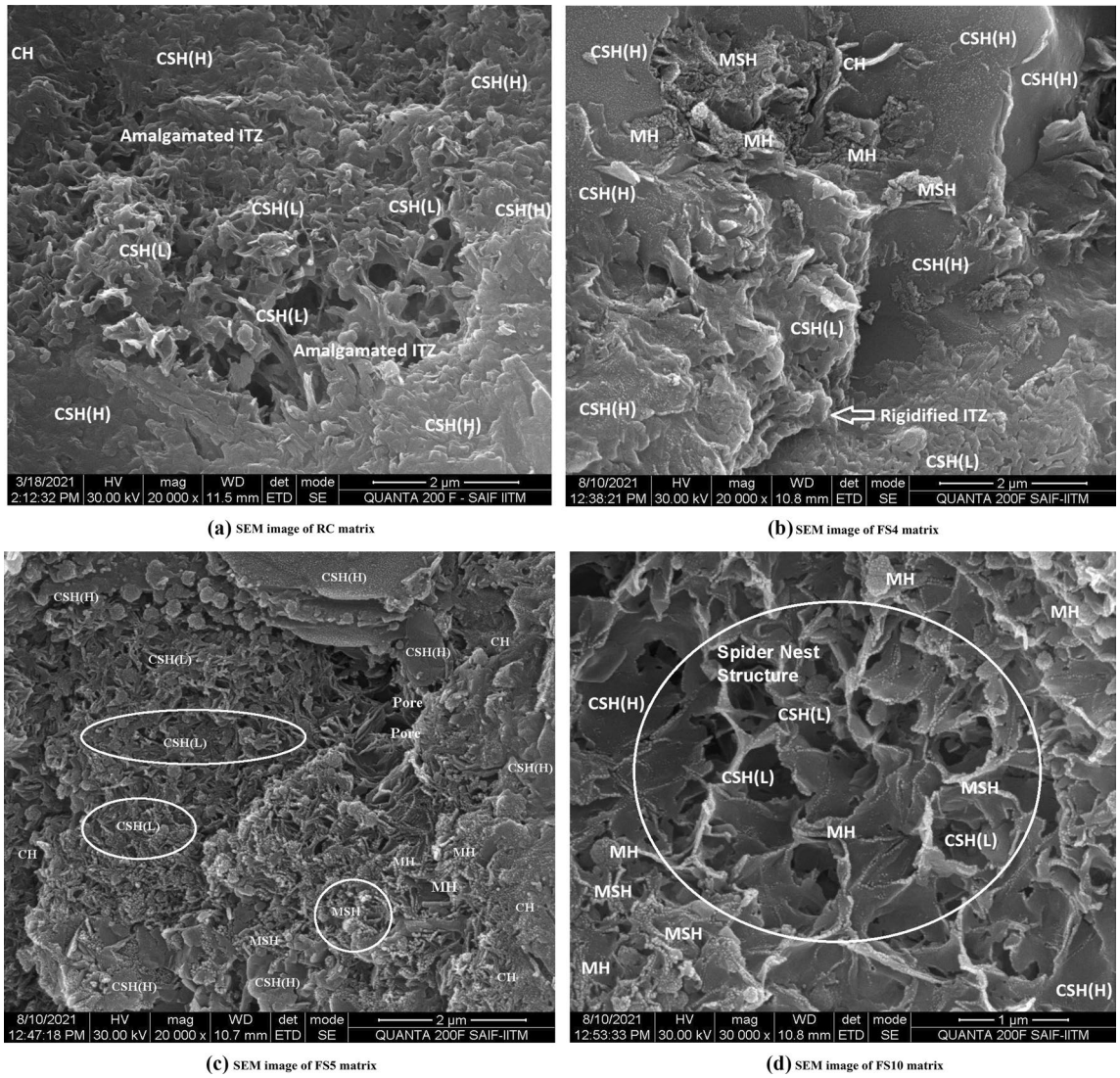

Fig. 10 **a** SEM image of the RC matrix. **b** SEM image of the FS4 matrix. **c** SEM image of the FS5 matrix. **d** SEM image of the FS10 matrix

Focusing on FS replacement, there is a slight increase of Cl^{--} ion penetration on increasing the FS. FS1, FS2, FS3 and FS4 mixes under very low chloride ion penetration. FS replacements at later ages are reduced due to the later hydration caused by Mg. FS replacements at later ages are reduced due to the later hydration caused by Mg. The all ages of FS5 mix ranges below low Cl^- ion penetration region. From the Fig. 9, FS10 has 2573, 2352 and 2092 Coulombs, respectively, on 28, 92 and 365 days. There are two major factors to increase the Cl^- ion in the slag matrix. Conductive ionic species such as Fe, Mg and Cr inside the slag allow a significant amount of Cl^- ion to penetrate. Continuous flow of 60 V current for 6 h in slag the matrix increases the temperature of the concrete by getting heated, thereby stimulating Cl^- ion penetration [47]. NMCM with FS10 is reported to maintain the Cl^- ion penetration in the moderate region. This is similar to the RC region of Cl^- ion penetration. WA and RCPT results are similar while increasing FS in concrete. The porous texture for water absorption and metal ingredients of slag are the reasons for the RCPT results.

Microstructural study

Information of microstructure confirms the high strength and durability of concrete. High magnification microscopy is performed up to 1–5 µm range (25 K magnification) using (FEI Quanta FEG 200). The samples are taken from 28 days of cured concrete. The cuts and curvature of hydrated particles are visualised. The C(A)SH are noted in two forms: CSH(H) and CSH(L) from the RC mix. CSH(H) shows a high-density region from the microscopic image and CSH(L) shows low density in the C(A)SH matrix. A dark

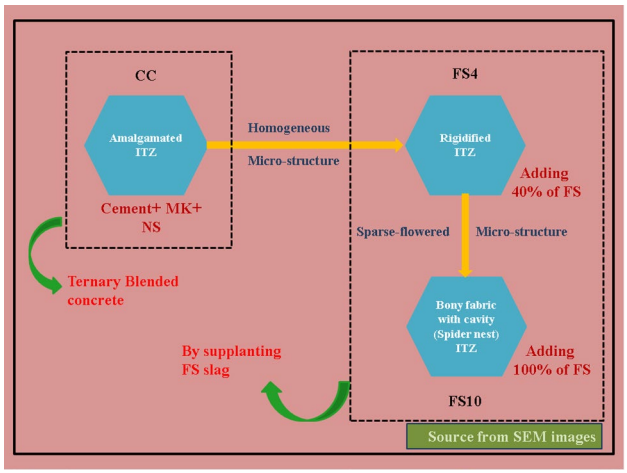

Fig. 11 Schematic ITZ transformation

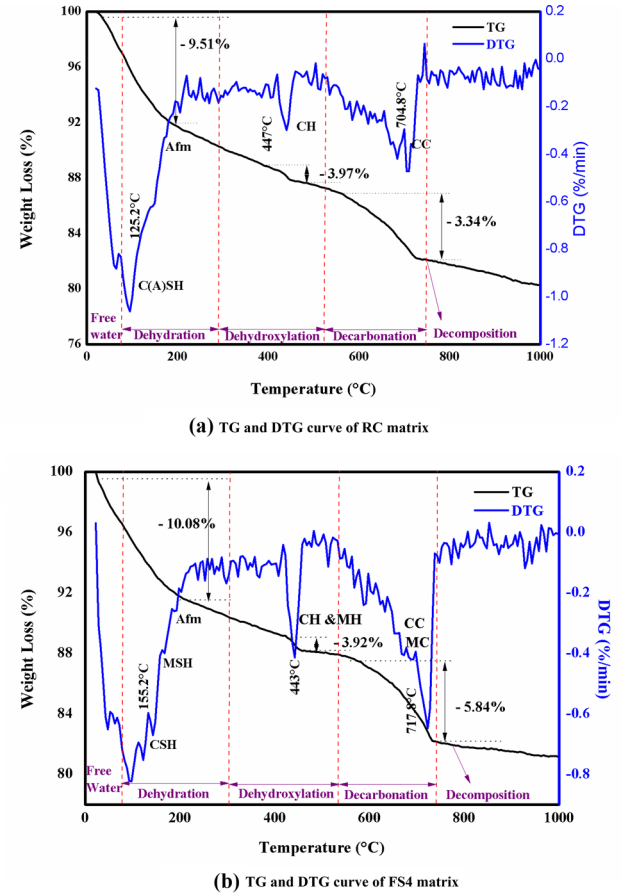

Fig. 12 **a** TG and DTG curve of the RC matrix. **b** TG and DTG curve of the FS4 matrix

spot of the image in the RC mix denotes the presence of CH. MK and NS incorporation will lead to form an amalgamated ITZ, which is predicted in Fig. 10a.

An enormous amount of CSH(H) is noted in Fig. 10 b) of the FS4 matrix. This represents that the cluster CSH(H) leads to superior strength performance. The interlocking action of Csand and FS refines a meso-capillary pore. Rigidified ITZ is predicted at the FS4 matrix. A negligible amount of MSH and MH are noted in a dotted form of the FS4 SEM image. Microstructural images of CSH(L) and brucite (MH) structure are similar to those of the current investigation [49]. The FS5 sample shows there is an initiation of homogeneity in the concrete SEM image. More CSH(L) and pores are found in Fig. 10 c.

MSH and MH are noted in the FS5 matrix. Adding 100% of FS leads to the formation of a *bony fabric with cavities* or *spider nest* shape structure as shown in Fig. 10d. A decrease in density and continuity of structure emphasize the strength and durability degradation of the FS10 cluster. MSH and Brucite are present in higher amounts in Fig. 10c, d. However, this Mg compound reduces the early hydration property of concrete. Figure 11 represent the schematic of ITZ transformation from the high magnified (1–2 µm) SEM report. Amalgamated ITZ is formed in RC. By partial supplanting of FS, there is a densification on ITZ. This shows that 40%-FS with 60%-Csand has a rigidified ITZ on the FS4 cluster. Above 50% of FS, addition causes pore visibility in Fig. 10c. FS10 has a discontinuity on the microstructures. Moreover, the ITZ of FS10 is in a sparse-flowered or spider nest shape.

Thermal study

The TG/DTG study on 28 days cured sample is tested. Figure 12 a, b represents the significant quantitative analysis of the hydroxyl and carbonation group. Investigation is done based on five different regions on thermal analysis. They are free water (up to 100 °C), dehydration (105–300 °C), dehydroxylation (300–550 °C), decarbonation (550–750 °C) and decomposition, respectively [34]. The mix RC has three intense peaks at 125.2, 447 and 704.8 °C in Fig. 12a. The dehydration region overlaps with the CSH, and Afm phase, where TG shows the loss of weight percentage as −9.51%. The second peak of the referral mix explains the amount of (CH) dehydroxylation is − 3.91%, and CC [$Ca(Co)_3$] is the third peak with a loss percentage of − 3.34%. The optimum mix (FS4) has multi-dehydration peaks due to the matrixes overlap of CSH, MSH and Afm [48].

The silicate hydroxide peaks fall at 155.2 °C, where the TG loss percentage is higher than RC (−10.08% mass loss). The higher loss percentage represents the presence of higher amounts of the silicate hydrate group. The hydroxylation peak falls at 443 °C, which is earlier and less intense than that of the referral mix. Moreover, − 3.92% of weight loss is recorded by the CH and MH functions. This reduces the hydroxide group in a matrix and has superior strength and

durability. This is similar to the SEM image of FS4, which has a lesser amount of CH and higher amount of CSH. The decarbonation region in Fig. 12b represents CC and MC at 717.8 °C [35, 36]. However, the intensity is slightly higher due to the presence of brucite in slag that reacts with carbonate ions [34]. Decarbonation is increased in the FS4 matrix than RC, where the weight loss percentages of RC and FS4 mixes are − 3.34% and − 5.84%, respectively [22, 36]. Nevertheless, Figs. 10d and 12b show that FS4 has less hydroxyl and a higher amount of CSH, which contributes significantly to the strength and durability of concrete.

Discussion and conclusion

Discussion

The overall discussions of this study on FS are briefed in this section. The strength, durability, microstructure and TG/DTG performances are as follows.

- The physico-chemical characteristic of FS matches the fine aggregate. MBV of FS is 0.5 and the grained slag lies between the zone II limit. EDS clarifies that Si and Al are significant and tiny amounts of Mg, Fe, Cr and Ca components are present in slag. Slump values of FS mixes are in the down face due to the porous nature of slag.
- The compressive strength property of FS4 has a 3.18% percentage increase over a referral mix on 28-day cured samples. This strength gain is due to NMCM in cement and *interlocking capacity* between FS and Csand. FS10 mix has 13.56% loss in strength,h but not below the target mean strength (TMS = 48.25 N/mm^2) of concrete at 28 days. Moreover, on FS replacements, the strength gain is shown in later ages due to the presence of Mg in slag.
- The UPV value of the FS4 mix has a 26.61% increase than the RC mix. The density and uniform dispersion of particles in the concrete lead to a rise in pulse velocity. Based on the UPV report, FS4 is excellent quality and FS10 is on good quality concrete.
- By increasing the slag composition, there is a decrease in WP depth, until 40% of FS replacement. The interlocking property of FS and Csand clog the WP. RC has better earlier resistance, whereas FS combinations show later age resistance to permeability depth.
- The WA of RC is low due to micro and nano pozzolans apprehending the capillary pores. Moreover, by replacing FS, there is an increase in water absorption. But FS4 mixes have 36.36% higher WA than RC. RCPT of the control mix lies on the very low range of chloride ion penetration. FS4 is slightly inferior to RCPT test results by an increase of 11.11% than RC.
- The microstructure of FS4 shows a higher amount of CSH and reduces CH content. The pozzolanic activity of Al–Si minerals makes a uniform microstructure in hetero concrete. ITZ are amalgamated and rigidified in the RC and FS4 cluster, respectively. These emphasize that the strength and durability of FS4 concrete is optimum. FS10 shows a spider nest-shaped CSH(L). MSH and MH are predicted from SEM images in the slag matrix.
- Thermal investigation portrays that CH is reduced in the FS4 mix than in the RC mix. Dehydration is slightly higher in FS4 due to a larger amount of silicate hydrate formation. All the test summaries of FS ratify it as fine aggregate in NMCM.

Conclusion and recommendation

Factual findings of ternary binder incorporating innocuous FS are pointed below.

- The detailed material characterisations of FS are amicable to utilize as fine aggregate in M40 concrete**.**
- Therefore, the workability of FS incorporated mix has a sliding face in concrete due to cavities of slag. The strength of 40% FS is escalated due to better interlocking action with Csand of 60%.
- The UPV, WA, WP, RCPT, and TG/DTG reports of the FS4 matrix support FS as a potential supplant of fine aggregate in concrete.
- Based on the current investigation, the FS4 mix is recommended for severely exposed structures with regime durability action. However, FS10 can be suggested for secondary structural applications such as partition walls, pavement parking and secondary beams.

Acknowledgements The authors acknowledge "Anna Centenary Research Fellowships Scheme Grant No: CFR/ACRF/19131191121/AR1" of CFR, Anna University, Chennai, Tamil Nadu, India.

Author contributions MN: Idea, experimental work, data analysis, work conducted, original draft writing, editing and revision. PV: Data analysis, draft formation, draft editing, revision, supervision and correction.

Declarations

Conflict of interest No conflicts or competing interest.

References

1. Schneider M, Romer M, Tschudin M, Bolio H (2011) Sustainable cement production–present and future. Cem Conc Res 41:642–650. https://doi.org/10.1016/j.cemconres.2011.03.019
2. Nandhini K, Ponmalar V (2018) Microstructural behaviour and flowing ability of slef-compacting concrete using micro- and nano-silica. Micro Nano Lett 13:1213–1218. https://doi.org/10.1049/mnl.2018.0105
3. El-Diadamony H, Amer AA, Sokkary TM, El-Hosney S (2018) Hydration and characteristics of metakaolin pozzolanic cement pastes. HBRC J 14:150–158. https://doi.org/10.1016/j.hbrcj.2015.05.005
4. Jamsheer AF, Kupwade-Patil K, Buyukozturk O, Bumajad A (2018) Analysis of engineered cement paste using silica nanoparticles and metakaolin using Si NMR, water adsorption and synchrotron X-ray Diffraction. Constr Build Mater 180:698–709. https://doi.org/10.1016/j.conbuildmat.2018.05.272
5. Dinakar P, Manu SN (2014) Concrete mix design for high strength self-compacting concrete using Metakaolin. Mater Design 60:661–668. https://doi.org/10.1016/j.matdes.2014.03.053
6. Lothenbach B, Karen Scrivener RD (2011) Supplementary cementitious materials. Cem. Conc. Res. 41:1244–1256. https://doi.org/10.1016/j.cemconres.2010.12.001
7. Dinakar P, Sahoo PK, Sriram G (2013) Effect of metakaolin content on the properties of high strength concrete. Int J Concrete Struct Mater 7(3):215–223. https://doi.org/10.1007/s40069-013-0045-0
8. Escalante JI, Sharp JH (2004) The chemical composition and microstructure of hydration products in blended cements. Cement Concr Compos 26:967–976. https://doi.org/10.1016/j.cemconcomp.2004.02.036
9. Muhd Norhasri MS, Hamidah MS, Fadzil M (2019) Inclusion of nano metaclayed as additive in ultra high performance concrete (UHPC). Constr Build Mater 201:590–598. https://doi.org/10.1016/j.conbuildmat.2019.01.006
10. Vishnu A, Ponmalar V (2021) Consistency, flow, strength and durability (CFSD) assessment on concrete using superior cementitious constituents. Roman J Mater 51(1):43–52
11. Potapov V, Efimenko Y, Fediuck R, Gorev D (2021) Effect of hydrothermal nano silica on the performances of cement concrete. Constr Build Mater 269:121307. https://doi.org/10.1016/j.conbuildmat.2020.121307
12. Hongjian Du, Suhuan Du, Liu X (2014) Durability performances of concrete with nano-silica. Constr Build Mater 73:705–712. https://doi.org/10.1016/j.conbuildmat.2014.10.014
13. Navarro-Blasco I, Perez-Nicolas M, Fernandez JM, Duran A, Sirera R, Alvarez JI (2014) Assessment of the interaction of polycarboxylate superplasticizers in hydrated lime pastes modified with nanosilica or metakaolin as pozzolanic reactives. Constr Build Mater 73:1–12. https://doi.org/10.1016/j.conbuildmat.2014.09.052
14. Mondal P, Shah SP, Marks LD, Gaitero JJ (2010) Comparative study of the effects of microsilica and nanosilica in concrete. J Transport Res Board 14:12
15. G. Quercia, H.J.H. Brouwers, 2010 Application of nano silica in concrete Mixture https://doi.org/10.13140/2.1.1797.5044.
16. Supit SWM, Shaikh FUA (2015) Durability properties of high volume fly ash concrete containing nano-silica. Mater Struct 48:2431–2445. https://doi.org/10.1617/s11527-014-0329-0
17. Tennis PD, Jennings HM (2000) A model for two types of calcium silicate hydrate in the microstructure of Portland cement pastes. Cem Conc Res 30:855–863. https://doi.org/10.1016/S0008-8846(00)00257-X
18. Manigandan N, Ponmalar V (2020) Ferrochrome slag and manufactured sand as fine aggregate replacement in concrete and mortar a Brief Review. Ind J Sci Technol. 13:2657–2667. https://doi.org/10.17485/IJST/v13i26.526
19. Arulmoly B, Konthesingha C, Nanayakkara A (2021) Performance evaluation of cement mortar produced with manufactured sand and offshore sand as alternatives for river sand. Constr Build Mater 297:123784. https://doi.org/10.1016/j.conbuildmat.2021.123784
20. Shen W, Yang Z, Cao L, Cao L, Liu Yi, Yang H, Zili Lu, Bai J (2016) Characterization of manufactured sand: Particle shape, surface texture and behavior in concrete. Constr Build Mater 144:595–601. https://doi.org/10.1016/j.conbuildmat.2016.03.201
21. Weiguo Shen YI, Liu LC, Yang Z, Zhou C, Pengtao He Zili L (2017) Mixing design and microstructure of ultra high strength concrete with manufactured sand. Constr Build Mater 143:312–321
22. Raja R, Vijayan P (2021) Investigations on mechanical characteristics and microstructural behavior of laterized high strength concrete mix. Arab J Sci Eng 46:10901–10916. https://doi.org/10.1007/s13369-021-05606-7
23. Nanthagopalan P, Santhanam M (2011) Fresh and hardened properties of self-compacting concrete produced with manufactured sand. Cement Concr Compos 33(3):353–358. https://doi.org/10.1016/j.cemconcomp.2010.11.005
24. Donza H, Cabrera O, Irassar EF (2002) High-strength concrete with different fine aggregate. Cem Conc Res 32(11):1755–1761. https://doi.org/10.1016/S0008-8846(02)00860-8
25. Siddique S, Chaudhary S, Shrivastava S, Gupta T (2019) Sustainable utilisation of ceramic waste in concrete: exposure to adverse conditions. J Clean Prod 210:246–255. https://doi.org/10.1016/j.jclepro.2018.10.231
26. International Chromium Development Association (ICDA), Activity Report 2017.
27. Dash MK, Patro SK (2018) Effect of water-cooled ferrochrome slag as fine aggregate on the properties of concrete. Constr Build Mater 177:457–466. https://doi.org/10.1016/j.conbuildmat.2018.05.079
28. Manoj Kumar Dash (2018) Sanjay kumar patro, performance assessment of ferrochrome slag as partial replacement of fine aggregate in concrete. Eur J Environ Civ Eng 25:1–20. https://doi.org/10.1080/19648189.2018.1539674
29. Al-Jabri K, Shoukry H, Kalil IS, Nasir S (2018) Reuse of waste ferrochrome slag in the production of mortar with Improved thermal and mechanical performance. J Mater Civ Eng 30(8):04018152. https://doi.org/10.1061/(ASCE)MT.1943-5533.0002345
30. Zahedul Islam M, Sohel KMA, Khalifa Al-Jabri A, Harthy Al (2021) Properties of concrete with ferrochrome slag as a fine aggregate at elevated temperatures. Case Stud Const Mater. 15:e00599. https://doi.org/10.1016/j.cscm.2021.e00599
31. Chandru P, Karthikeyan J, Sahu AK, Ketan Sharma C (2021) Some durability characteristics of ternary blended SCC containing crushed stone and induction furnace slag as coarse aggregate. Constr Build Mater 270:121483. https://doi.org/10.1016/j.conbuildmat.2020.121483
32. Fares AI, Sohel KMA, Abdullah Al-Mamun K (2021) Characteristics of ferrochrome slag aggregate and its uses as a green material in concrete. Constr Build Mater 294:123552. https://doi.org/10.1016/j.conbuildmat.2021.123552
33. Dash MK, Patro SK, Rath AK (2016) Sustainable use of industrial-waste as partial replacement of fine aggregate for preparation of concrete. Int J Sustain Built Environ 5:484–516. https://doi.org/10.1016/j.ijsbe.2016.04.006

34. Karen Scrivener, (2016) A practical guide to microstructural analysis of cementitious materials, Swizerland
35. Borges PHR, Costa JO, Milestone NB, Lynsdale CJ, Roger E (2010) Streatfield, Carbonation of CH and C-S–H in composite cement pastes containing high amounts of BFS. Cem. Conc. Res. 40:284–292. https://doi.org/10.1016/j.cemconres.2009.10.020
36. Hay R, Otchere C, Kashwani G, Celik K (2021) Recycling carbonated reactive magnesium cement (RMC) as a building material. J cleaner prod 320:128838. https://doi.org/10.1016/j.jclepro.2021.128838
37. IS 12269:1987. R2013. Ordinary Portland Cement 53 Grade – Specification, Bureau of Indian Standards, New Delhi, India.
38. IS 2386–3:1963. Methods of Test for Aggregate for Concrete - part 3: Specific Gravity, Density, Voids, Absorption and Bulking, Bureau of Indian Standards, New Delhi, India.
39. BS EN 933–9:2010. Test for geometrical properties of aggregate : Assesement of finess Methylene blue test, British Standard Institution.
40. IS 10262:2009. R2019. Concrete Mix Proportioning – Guidelines, Bureau of Indian Standards, New Delhi, India.
41. IS 383:1970. R2016. Specification for Coarse and Fine aggregate from Natural Sources for Concrete, Bureau of Indian Standards, New Delhi, India.
42. IS 4925:2004. Concrete Batching and Mixing Plant – Specification, Bureau of Indian Standards, New Delhi, India.
43. IS 11311–1:1992. Method of Non-destructive testing of concret, Part 1: Ultrasonic pulse velocity. Bureau of Indian Standards, New Delhi, India.
44. IS 3805:1965. Method of Test for Permeability of Cement Mortar and Concrete. Bureau of Indian Standards, New Delhi, India.
45. ASTM C642:2013. Standard Test Method for Density, Absorption, and Voids in Hardened Concrete, ASTM International, West Conshohocken, PA.
46. ASTM C1202:2019. Standard Test Method for Electrical Indication of Concrete's Ability to Resist Chloride Ion Penetration, ASTM International, West Conshohocken, PA.
47. Manu Santhanam (2019) Durability issues in concrete – Part 1. NPTEL-NOC IITM, https://www.youtube.com/watch?v=2npeWrad0TU
48. Nieda D, Enemark-Rasmussenc K, L'Hopital E, Skibsted J, Lothenbachb B (2016) Properties of magnesium silicate hydrate (M-S-H). Cem Conc Res 79:323–332. https://doi.org/10.1016/j.cemconres.2015.10.003
49. Tekina I, Dirikolu I, Gokce HS (2021) A regional supplementary cementitious material for the cement industry: Pistachio shell ash. J clean prod 285:124810. https://doi.org/10.1016/j.jclepro.2020.124810
50. Mannigandan N, Ponmalar V (2022) M5 investigation on ternary binder incorporated with ferrochrome slag aggregate in concrete. Appl Nano sci. https://doi.org/10.1007/s13204-022-02615-2
51. IS 1199–2: 2018. Fresh Concrete - Methods of Sampling, Testing and Analysis Bureau of Indian Standards, New Delhi, India.

Authors and Affiliations

Manigandan Nagarajan[1] · **Ponmalar Vijayan**[1]

✉ Ponmalar Vijayan
ponmalar_v@annauniv.edu

Manigandan Nagarajan
authormanigandan@gmail.com;
manigandan.civil.phd@gmail.com

[1] Division of Structural Engineering, Department of Civil Engineering, College of Engineering Guindy, Anna University, Chennai, Tamil Nadu, India